Journal of NUCLEAR SCIENCE and TECHNOLOGY, Vol. 42, No. 10, p. 897–902 (October 2005)

TECHNICAL REPORT

Helium Production in Solid Target and Metallic Window Materials Irradiated with Intermediate and High Energy Protons

Cornelis H. M. BROEDERS and Alexander Yu. KONOBEYEV*

Institut für Reaktorsicherheit, Forschungszentrum Karlsruhe GmbH, 76021 Karlsruhe, Germany

(Received May 16, 2005 and accepted in revised form August 12, 2005)

The helium isotope formation cross-section has been obtained for iron, tantalum and tungsten irradiated with protons at energies from the reaction threshold up to several GeV. The cross-section evaluation has been performed using the results of model calculations and by the analysis of available experimental data.

The numerical calculations were carried out using the modified ALICE code and the CASCADE/INPE code.

KEYWORDS: protons, intermediate energies, high energies, helium 4, helium 3 isotope production, cross-section, evaluation, iron, tantalum, tungsten

I. Introduction

The study of helium production in nuclear reactions induced by intermediate and high energy protons is an important part of the investigation of radiation durability of materials designed for accelerator driven systems (ADS), neutron generators and other emerging nuclear energy systems.

Evaluation of the helium production rate in irradiated materials is hindered by the significant spread of experimental helium formation cross-sections and deficiencies in the model calculations. For example the modern measurements of helium yield for iron[1,2] give the values, which are different in 1.8 times. Despite of progress in development of theoretical methods of calculation, their use encounters the problem of the correct description of the non-equilibrium ^{3}He- and ^{4}He-emission using the pre-compound exciton model and the intranuclear cascade model.[3] Other problem is the simulation of the equilibrium emission of helium isotopes at high energies by the intranuclear cascade evaporation model, which assumes the use of simplified approaches for describing the particle emission rates.[3]

The goal of this work is analysis and the evaluation of the helium production cross-section in iron, tungsten and tantalum irradiated with protons at energies from the reaction threshold up to several GeV. This energy range covers all possible proton irradiation conditions in the ADS systems[4–7] and neutron generators.[8,9] The calculations have been performed up to the maximal energy 25 GeV, where the experimental data for helium production are available.

II. Brief Description of the Method of Helium Production Cross-Section Evaluation

Helium production cross-section has been calculated as a sum of cross-sections of ^{4}He (σ_α) and ^{3}He ($\sigma_{^3\mathrm{He}}$) formation

$$\sigma_{\mathrm{He}} = \sigma_\alpha + \sigma_{^3\mathrm{He}}. \quad (1)$$

The analysis of the methods of calculation used in popular computer codes has shown,[3] that the helium production cross-section can be obtained with a good accuracy using the models describing the composite particle emission implemented in the ALICE/ASH code[10,11] and in the DISCA code.[3,12–14] The application of the ALICE/ASH code is limited by the energy of projectiles up to 150–200 MeV and the DISCA code to ~800 MeV. These energies are insufficient for the analysis of the helium yield in materials irradiated with high energy protons in different emerging nuclear energy systems. Furthermore the codes indicated cannot be used for the analysis of entire bulk of the experimental helium production cross-sections, which are available at low, intermediate and high energies. Such analysis is necessary for the definition of consistent sets of experimental data and elimination of uncertainty in values of helium production cross-section arising from the spread of data obtained in different experiments.

In the present work the ^{4}He- and ^{3}He-production cross-sections are calculated using the CASCADE/INPE code[12,15–19] implementing the intranuclear cascade evaporation model. The model is applicable for the calculation in the energy region of primary particles up to several tens of GeV.[17] The specific features of the model include the approximation of the nuclear density by the continuous Woods-Saxon distribution, the use of the "time-like" Monte Carlo technique and the consideration of the effect of nuclear density depletion due to the fast nucleon emission. The model is described in details in Refs. 15, 20, 21).

The contribution of the non-equilibrium emission in the ^{4}He- and ^{3}He-production cross-sections is calculated using the approximate approach close to the model of "nuclear bond breakdown".[22,23] Considering the ^{3}He- and α-clusters as a stable nucleon association located on a periphery of the nucleus[20] it is easy to show, that at high projectile energies the number of clusters knocked-out from the nucleus is proportional to the number of nucleons emitted on the cascade stage of the reaction and the square of the nucleus radius. This implies, that the non-equilibrium component of the ^{4}He- and ^{3}He-production cross-sections at the high energies of projectiles can be evaluated as follows:

*Corresponding author, Tel. +49-07247-82-2638,
E-mail: konobeev@irs.fzk.de

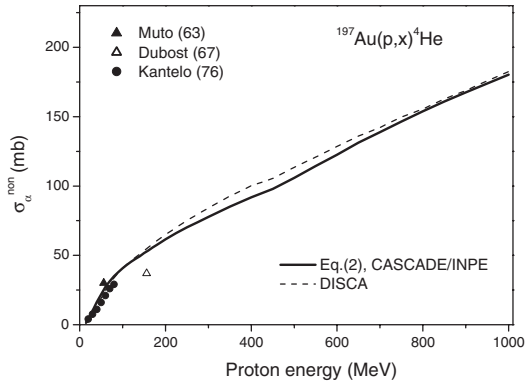

Fig. 1 The fraction of the ^{4}He-production cross-section concerning the non-equilibrium emission of ^{4}He nuclei calculated using the CASCADE/INPE code and Eq. (2) (solid line) and calculated by the nuclear bond breakdown approach[22] using the DISCA code (dashed line) for ^{197}Au irradiated with protons. Experimental points are from Refs. 30–32).

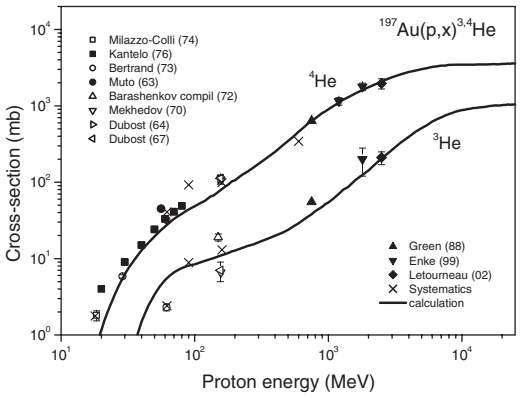

Fig. 2 The ^{4}He- and ^{3}He-production cross-sections for ^{197}Au calculated by the ALICE/ASH code and the CASCADE/INPE code, evaluated by the systematics[3,42] and measured.[2,20,30–32,36–41] The experimental cross-section[2] at 1.2 GeV is corrected for the ^{3}He contribution.[3]

$$\sigma_x^{non}(E) = \sigma_{non}(E)\gamma_x N_{casc}(E), \quad (2)$$

where $\sigma_{non}(E)$ is the cross-section for nonelastic interactions of the primary particle with the kinetic energy E and the nucleus, N_{casc} is the average number of nucleons emitted from the nucleus during the cascade (fast) stage of the reaction, γ_x is the energy independent parameter, which value should be defined from the analysis of experimental data or from independent theoretical calculations, "x" refers to the type of the cluster knocked out.

In the present work the number of cascade nucleons N_{casc} was calculated by the CASCADE/INPE code. The γ_x value has been defined using the result of the ALICE/ASH code calculation at the primary proton energy around 100 MeV. The models describing the complex particle emission[24–28] implemented in the ALICE/ASH code have been tested and approved at this energy in many works.[3,10,11,26–29]

Figure 1 shows the non-equilibrium component of the ^{4}He-production cross-section σ_α^{non} calculated using Eq. (2) and obtained using the nuclear bond breakdown model by the DISCA code for ^{197}Au. The parameters of the model[22,23] are N_0=0.104, m_0=0.06. The experimental data from Refs. 30–32) are shown. There is a reasonable agreement between the σ_α^{non} values calculated by different approaches and the available experimental data.

In the present work Eq. (2) has been used to obtain the contribution of the non-equilibrium emission in the total ^{4}He- and ^{3}He-production cross-sections at intermediate and high energies of incident protons. At proton energies below 100 MeV the values of σ_α^{non} and $\sigma_{^3\mathrm{He}}^{non}$ have been calculated by the ALICE/ASH code. The contribution of the equilibrium emission in the ^{4}He- and ^{3}He-production cross-sections has been obtained using the CASCADE/INPE code. The obtained value of the γ parameter, Eq. (2) for ^{4}He-emission is equal to 4.75×10^{-2} for ^{56}Fe, 2.3×10^{-2} for ^{181}Ta, from 2.58×10^{-2} to 2.31×10^{-2} for various tungsten isotopes and 1.85×10^{-2} for ^{197}Au. The value of γ for ^{3}He is equal to 8.57×10^{-3} for ^{56}Fe, 4.49×10^{-3} for ^{181}Ta, from 5.3×10^{-3} to 4.34×10^{-3} for tungsten isotopes and 3.81×10^{-3} for ^{197}Au.

The total reaction cross-section for protons σ_{non} at high energies has been obtained using the evaluated data from Ref. 33). At low and intermediate energies the σ_{non} value was calculated by the optical model with the potential from Ref. 34) and with the help of the MCNPX code built-in routine.[35]

The example of the ^{4}He- and ^{3}He-production cross-sections calculated for ^{197}Au is shown in **Fig. 2**. There is a rather good agreement between the calculated cross-sections and experimental data[2,20,30–32,36–41] in the whole energy region, where the measured data are available. The agreement is also observed with the values of cross-section predicted by the empirical systematics,[3,42] except the calculated ^{4}He-production cross-section at 18 and 90 MeV and ^{3}He-production cross-section at 62 MeV.

III. Results and Discussion

The helium production cross-section has been calculated for ^{56}Fe, ^{181}Ta and tungsten isotopes ^{180}W, ^{182}W, ^{183}W, ^{184}W and ^{186}W.

Figure 3 shows the ^{4}He- and ^{3}He-production cross-sections for ^{56}Fe calculated by the ALICE/ASH and CASCADE/INPE codes, the cross-sections evaluated by systematics[3,42] and measured data.[1,20,40,43–48] All measurements refer to natural iron, except the data[47] for ^{56}Fe. Data from Refs. 37, 49) are not shown because the measurement has been performed with a high value of the cutoff energy for ^{4}He (14.26 MeV). The calculations were carried out using the ALICE/ASH code up to 200 MeV and by the CASCADE/INPE code in a whole energy region where experimental data exist. For the comparison the available data from ENDF/B-VI (Proton Sublibrary) and from JENDL-HE are shown. There is reasonable agreement between the calculated ^{4}He-production cross-section, systematics and experimental data. The agreement for ^{3}He is worse, and calculations as a whole overestimate the measured cross-sections.

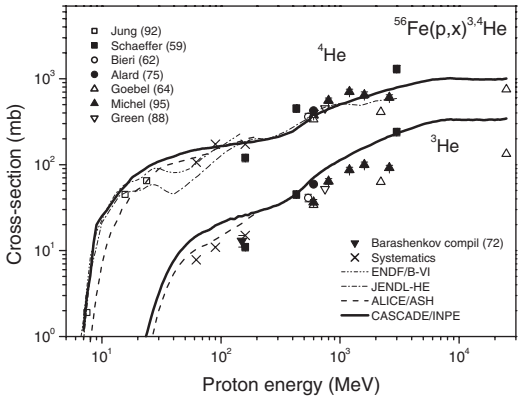

Fig. 3 The ^{4}He- and ^{3}He-production cross-sections for ^{56}Fe calculated by the ALICE/ASH code and the CASCADE/INPE code, evaluated by the systematics[3,42] and measured.[1,20,40,43–48] The ^{4}He-production cross-sections from ENDF/B-VI and JENDL-HE are shown.

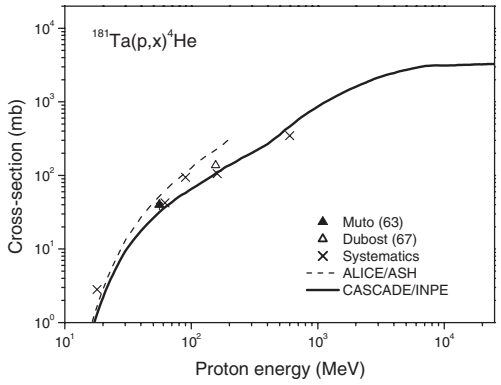

Fig. 4 The ^{4}He-production cross-section for ^{181}Ta calculated by the ALICE/ASH code and the CASCADE/INPE code, evaluated by the systematics[3,42] and measured.[30,31] The measured yield of ^{4}He having isotropic angular distribution[31] was added by the value obtained[31] for heavy nuclei (Au, Bi) relating to anisotropic ^{4}He-emission.

One should note, that the non-equilibrium component of helium isotope production cross-section has been calculated using the global systematics of parameters of the pre-compound model used in the ALICE/ASH code. The systematics has been obtained in Refs. 10, 11) from the analysis of experimental data on the complex particle emission in nuclear reactions. The agreement between the results of calculations for ^{3}He can be improved by the appropriate choice of the pre-compound model parameters. From other side the observed difference does not essentially effect on the value of the total helium production cross-section because the contribution of ^{3}He is relatively small. The systematic deviation of the calculated and measured cross-section for the ^{3}He formation has been eliminated in the present work with the evaluation of the helium production cross-section.

Figures 4–6 show the ^{4}He- and total helium production cross-sections for ^{181}Ta calculated using the ALICE/ASH and CASCADE/INPE codes, measured in Refs. 2, 30, 31, 50) and predicted by systematics. Experimental data for ^{3}He-production are not available. The detail view of the high energy region is given in Fig. 6. There is the good agreement between calculations and experimental data.

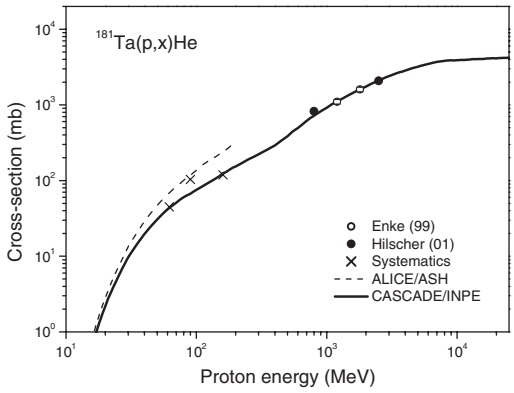

Fig. 5 The helium production cross-section ($\sigma_{^{3}He}+\sigma_{\alpha}$) for ^{181}Ta calculated by the ALICE/ASH code and the CASCADE/INPE code, evaluated by the systematics[3,42] and measured.[2,50]

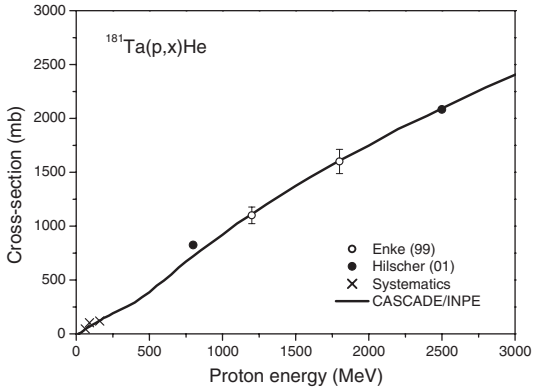

Fig. 6 Detail view of the helium production cross-section for ^{181}Ta calculated at energies up to 3 GeV.

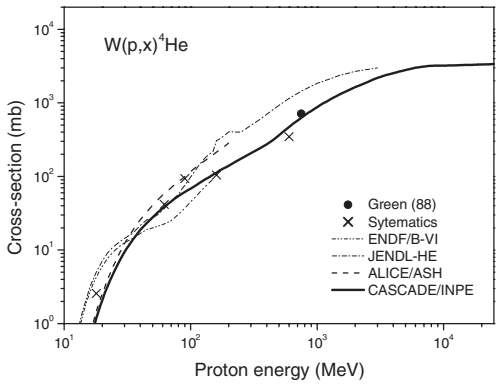

Fig. 7 The ^{4}He-production cross-section for natural tungsten calculated by the ALICE/ASH code and the CASCADE/INPE code, evaluated by the systematics,[3,42] measured[40] and taken from ENDF/B-VI and JENDL-HE.

The results obtained for natural tungsten are shown in **Figs. 7–9**. The good agreement is observed between the

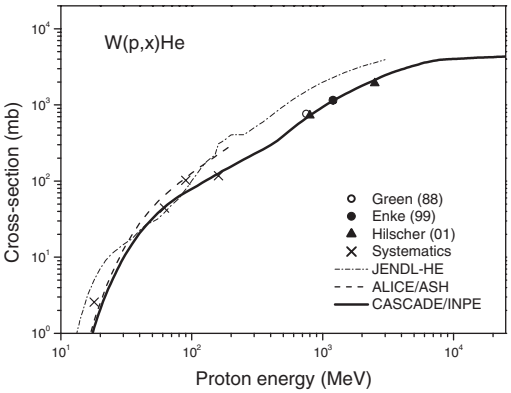

Fig. 8 The helium production cross-section for natural tungsten calculated by the ALICE/ASH code and the CASCADE/INPE code, evaluated by the systematics,[3,42] measured[2,40,50] and taken from JENDL-HE.

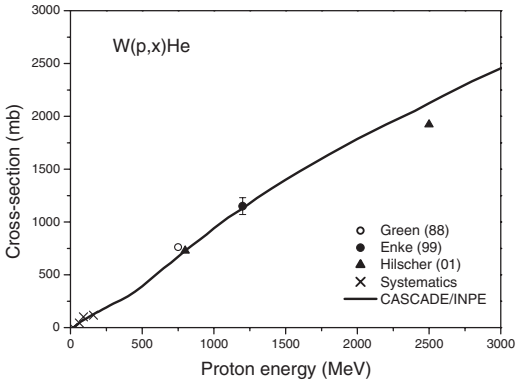

Fig. 9 Detail view of the helium production cross-section for tungsten calculated at energies up to 3 GeV.

Table 1 The evaluated helium production cross-section for iron, ^{181}Ta and tungsten irradiated with protons
The cross-sections between the energy points shown should be found by the linear(x)–log(y) interpolation at energies below 14 MeV, and by the linear–linear interpolation at energies above 14 MeV.

Proton energy (MeV)	Cross-section (mb)			Proton energy (MeV)	Cross-section (mb)		
	^{nat}Fe	^{181}Ta	^{nat}W		^{nat}Fe	^{181}Ta	^{nat}W
4	4.24×10^{-6}	1.03×10^{-9}	2.86×10^{-5}	350	246	346	353
5	6.90×10^{-4}	9.94×10^{-8}	5.88×10^{-5}	400	266	396	399
6	0.112	4.15×10^{-6}	2.26×10^{-4}	450	300	446	446
8	4.88	6.84×10^{-4}	1.86×10^{-3}	500	335	496	493
10	21.2	1.70×10^{-2}	1.43×10^{-2}	550	370	548	543
12	31.4	0.135	8.85×10^{-2}	600	406	598	593
14	43.4	0.548	0.391	650	435	649	646
16	45.3	1.42	1.20	700	464	700	698
18	50.4	2.82	2.57	750	481	751	762
20	55.4	3.98	4.18	800	507	824	805
22	60.6	5.22	5.92	850	525	836	848
24	65.9	6.52	7.24	900	544	870	891
26	75.1	8.09	8.69	950	561	906	934
28	82.4	9.66	10.3	1,000	580	940	978
30	91.2	11.7	12.2	1,200	634	1,100	1,150
35	102	16.9	17.1	1,500	712	1,370	1,350
40	109	23.4	22.8	2,000	807	1,750	1,680
50	121	37.2	34.3	2,500	895	2,080	1,920
60	131	50.2	46.2	3,000	966	2,400	2,310
70	141	61.3	57.1	4,000	1,060	2,840	2,860
80	149	72.0	68.2	5,000	1,150	3,200	3,260
90	165	82.4	79.3	6,000	1,210	3,480	3,580
100	172	92.4	89.5	7,000	1,240	3,710	3,790
120	181	113	111	8,000	1,250	3,830	3,920
150	188	144	144	10,000	1,250	3,910	4,010
200	201	195	202	15,000	1,230	4,040	4,170
250	213	246	254	20,000	1,230	4,130	4,240
300	226	296	306	25,000	1,250	4,210	4,330

σ_α and σ_{He} values calculated by the ALICE/ASH and CASCADE/INPE codes and the experimental data.[2,40,50]

The calculations performed make it possible to describe basic properties of the helium production cross-section. For the heavy nuclei (Ta, W, Au) the non-equilibrium emission of ^{4}He and ^{3}He nuclei gives the main contribution in the helium yield at energies below 80–100 MeV. With an increase of the primary proton energy the contribution of the non-equilibrium emission in the σ_{He} cross section decreases to 50% at the energy 300 MeV and to ~20% at energy 3 GeV. At the energy above 3 GeV the non-equilibrium fraction of the helium production cross-section barely

changes. The total helium production cross section is almost linear function of the primary particle energy in the range from 200 MeV to 1.5 GeV. At the energy above 1.5 GeV the growth of the cross-section is slowed down and the σ_{He} value reaches "saturation" at the energy 8–10 GeV. In the energy region above 10 GeV, the cross-section does not change noticeably. For iron the energy dependence of the σ_{He} cross-section is more complex function. As for heavy nuclei, the σ_{He} value reaches the saturation at energies 5–6 GeV.

The results of calculations and available experimental data have been used for the evaluation of the helium production cross-section for iron, tantalum and tungsten. A rather small correction of theoretical curves was carried out to avoid the systematic difference between calculations and experiments.

The evaluated helium production cross-sections are shown in **Table 1**. The data obtained can be used for the evaluation of the helium production rates in iron, tantalum and tungsten irradiated with protons with energies from several MeV up to 25 GeV.

Returning to the question about the difference in the helium production cross-sections measured for iron irradiated with 1.2 GeV-proton in Ref. 1) (792 mb) and in Ref. 2) (440 mb), one should note, that the evaluated value of the σ_{He} cross-section (634 mb, Table 1) is approximately on the middle. The data obtained in Ref. 2) seem underestimated because of the high value of minimal ^{4}He energy (10.8 MeV) adopted for the measurements. Calculations show that the energy 10.8 MeV lies in the region of the evaporation peak in the ^{4}He-emission spectrum, and the fraction of the ^{4}He nuclei emitted with energies below 10.8 MeV appears significant.

IV. Conclusion

The helium production cross-section has been evaluated for iron, ^{181}Ta and tungsten at proton energies from several MeV to 25 GeV.

The results of model calculations and available experimental data have been used for the cross-section evaluation. Main calculations have been carried out using the CASCADE/INPE code. The non-equilibrium component of the ^{4}He- and ^{3}He-production cross-sections has been obtained by Eq. (2). The value of the γ parameter was defined using the results of the ALICE/ASH code calculations.

The evaluated data are shown in Table 1. Data can be used for the calculation of the helium production rate in iron, tantalum and tungsten irradiated in various high energy units.

References

1) R. Michel, M. Gloris, H.-J. Lange, I. Leya, M. Lüpke, U. Herpers, B. Dittrich-Hannen, R. Rösel, Th. Schiekel, D. Filges, P. Dragovitsch, M. Sute, H.-J. Hofmann, W. Wölfli, P. W. Kubik, H. Baur, R. Wieler, *Nucl. Instrum. Methods*, **B103**, 183 (1995).
2) M. Enke, C.-M. Herbach, D. Hilscher, U. Jahnke, O. Schapiro, A. Letourneau, J. Galin, F. Goldenbaum, B. Lott, A. Péghaire, D. Filges, R.-D. Neef, K. Nünighoff, N. Paul, H. Schaal, G. Sterzenbach, A. Tietze, L. Pienkowski, *Nucl. Phys.*, **A657**, 317 (1999).
3) C. H. M. Broeders, A. Yu. Konobeyev, *Nucl. Instrum. Methods*, **B234**, 387 (2005).
4) A European Roadmap for Developing Accelerator Driven Systems (ADS) for Nuclear Waste Incineration. The European Technical Working Group on ADS, April 2001, Ente per le Nuove tecnologie, l'Energia e l'Ambiente (ENEA), April 2001, http://fachp1.ciemat.es/references/roadmap_eu_xads.pdf
5) TRADE Final Feasibility Report—March 2002 by the Working Group on TRADE: TRiga Aceelerator Driven Experiment.
6) Multi-Purpose Hybrid Research Reactor for High-Tech Applications. A European XT-ADS at Mol, http://www.sckcen.be/myrrha/
7) Accelerator-Driven Transmutation Experimental Facility. High Intensity Proton Accelerator Project. JAERI and KEK Joint Project, http://j-parc.jp/Transmutation/en/ads.html
8) European Spallation Source (ESS) Project, Forschungszentrum Jülich, http://www.fz-juelich.de/ess/
9) Spallation Neutron Source. A US Department of Energy Multilaboratory Project, http://www.sns.gov/
10) A. Yu. Konobeyev, Yu. A. Korovin, P. E. Pereslavtsev, *Code ALICE/ASH for Calculation of Excitation Functions, Energy and Angular Distributions of Emitted Particles in Nuclear Reactions*, Obninsk Institute of Nuclear Power Engineering, (1997).
11) A. I. Dityuk, A. Yu. Konobeyev, V. P. Lunev, Yu. N. Shubin, *New Advanced Version of Computer Code ALICE-IPPE*, INDC(CCP)-410, (1998).
12) *International Codes and Model Intercomparison for Intermediate Energy Activation Yields*, NSC/DOC(97)-1, (1997), http://www.nea.fr/html/science/docs/1997/nsc-doc97-1/
13) A. Yu. Konobeyev, Yu. A. Korovin, *Kerntechnik*, **63**, 124 (1998).
14) A. Yu. Konobeyev, Yu. A. Korovin, P. E. Pereslavtsev, U. Fischer, U. von Möllendorff, *Nucl. Sci. Eng.*, **139**, 1 (2001).
15) V. S. Barashenkov, B. F. Kostenko, A. M. Zadorogny, *Nucl. Phys.*, **A338**, 413 (1980).
16) V. S. Barashenkov, Le Van Ngok, L. G. Levchuk, Zh. Zh. Musulmanbekov, *et al.*, *CASCADE—The Code Package for the Simulation of Nuclear Processes Induced by High Energy Particles and Nuclei in Gaseous and Condensed Matter*, JINR R2-85-173, Dubna, (1985).
17) V. S. Barashenkov, *Comput. Phys. Commun.*, **126**, 28 (2000).
18) V. S. Barashenkov, A. Yu. Konobeyev, Yu. A. Korovin, V. N. Sosnin, *At. Energy*, **87**, 742 (1999).
19) A. Yu. Konobeyev, Yu. A. Korovin, M. Vecchi, *Kerntechnik*, **64**, 216 (1999).
20) V. S. Barashenkov, V. D. Toneev, *Interaction of High Energy Particles and Atomic Nuclei with Nuclei*, Atomizdat, Moscow, (1972).
21) V. S. Barashenkov, *et al.*, *Usp. Fiz. Nauk*, **109**, 91 (1973).
22) F. P. Denisov, V. N. Mekhedov, *Nuclear Reactions at High Energies*, Atomizdat, Moscow, (1972).
23) A. Yu. Konobeyev, Yu. A. Korovin, *J. Nucl. Mater.*, **195**, 286 (1992).
24) A. Iwamoto, K. Harada, *Phys. Rev.*, **C26**, 1821 (1982).
25) K. Sato, A. Iwamoto, K. Harada, *Phys. Rev.*, **C28**, 1527 (1983).
26) A. Yu. Konobeyev, Yu. A. Korovin, *Kerntechnik*, **59**, 72 (1994).

27) A. Yu. Konobeyev, V. P. Lunev, Yu. N. Shubin, *Acta Phys. Slovaca*, **45**, 705 (1995).
28) A. Yu. Konobeyev, Yu. A. Korovin, *Kerntechnik*, **61**, 45 (1996).
29) Yu. N. Shubin, V. P. Lunev, A. Yu. Konobeyev, A. I. Dityuk, *Cross-Section Library MENDL-2 to Study Activation and Transmutation of Materials Irradiated by Nucleons of Intermediate Energies*, INDC(CCP)-385, (1995).
30) J. Muto, H. Iton, K. Okano, N. Shiomi, K. Fukuda, Y. Omori, M. Kinara, *Nucl. Phys.*, **47**, 19 (1963).
31) H. Dubost, B. Gatty, M. Lefort, J. Peter, X. Tarrago, *J. Phys.*, **28**, 257 (1967).
32) M. V. Kantelo, J. J. Hogan, *Phys. Rev.*, **C13**, 1095 (1976).
33) V. S. Barashenkov, A. Polanski, *Electronic Guide for Nuclear Cross Sections*, JINR E2-94-417, Dubna, (1994), http://doc.cern.ch/tmp/convert_SCAN-9503228.pdf
34) A. J. Koning, J. P. Delaroche, *Nucl. Phys.*, **A713**, 231 (2003).
35) J. S. Hendricks, G. W. Mckinney, L. S. Waters, T. L. Roberts, *et al.*, *MCNPX Extensions. Version 2.5.0*, LA-UR-04-0570, (2004).
36) L. Milazzo-Colli, G. M. Braga-Marcazzan, M. Milazzo, C. Signorini, *Nucl. Phys.*, **A218**, 274 (1974).
37) F. E. Bertrand, R. W. Peelle, *Phys. Rev.*, **C8**, 1045 (1973).
38) B. N. Mekhedov, V. N. Mekhedov, (1970), cited by Ref. 20).
39) H. Dubost, M. Lefort, J. Peter, X. Tarrago, *Phys. Rev.*, **136**, B1618 (1964).
40) S. L. Green, W. V. Green, F. H. Hegedus, M. Victoria, W. F. Sommer, B. M. Oliver, *J. Nucl. Mater.*, **155/157**, 1350 (1988).
41) A. Letourneau, A. Böhm, J. Galin, B. Lott, A. Péghaire, M. Enke, C.-M. Herbach, D. Hilscher, U. Jahnke, V. Tishchenko, D. Filges, F. Goldenbaum, R. D. Neef, K. Nünighoff, N. Paul, G. Sterzenbach, L. Pienkowski, J. Tõke, U. Schröder, *Nucl. Phys.*, **A712**, 133 (2002).
42) A. Yu. Konobeyev, T. Fukahori, O. Iwamoto, *Neutron and Proton Nuclear Data Evaluation for ^{235}U and ^{238}U at Energies up to 250 MeV*, JAERI-Research 2002-028, (2002).
43) P. Jung, *Proc. Int. Conf. on Nuclear Data for Science and Technology*, Jülich, Germany, May 13–17, 1991, Springer-Verlag, p. 352 (1991).
44) O. A. Schaeffer, J. Zähringer, *Z. Naturforsch.*, **A13**, 346 (1958).
45) O. A. Schaeffer, J. Zähringer, *Phys. Rev.*, **113**, 674 (1959).
46) von R. H. Bieri, W. Rutsch, *Helv. Phys. Acta*, **35**, 553 (1962).
47) J. P. Alard, A. Baldit, R. Brun, J. P. Costilhes, J. Dhermain, J. Fargeix, L. Fraysse, J. Pellet, G. Roche, J. C. Tamain, *Nuovo Cimento*, **A30**, 320 (1975).
48) K. Goebel, H. Schultes, J. Zähringer, *Production Cross Sections of Tritium and Rare Gases in Various Target Elements*, CERN 64-12, (1964), cited by Ref. 20).
49) F. E. Bertrand, R. W. Peelle, EXFOR O0294001.
50) D. Hilscher, C.-M. Herbach, U. Jahnke, V. Tishchenko, M. Enke, D. Filges, F. Goldenbaum, R.-D. Neef, K. Nünighoff, N. Paul, H. Schaal, G. Sterzenbach, A. Letourneau, A. Böhm, J. Galin, B. Lott, A. Péghaire, L. Pienkowski, *J. Nucl. Mater.*, **296**, 83 (2001).